ADVANCED SUSTAINABLE SYSTEMS
www.advsustainsys.com

GrafeoPlad Palladium: Insight on Structure and Activity of a New Catalyst Series of Broad Scope

Matteo Formenti, Maria Pia Casaletto, Giampaolo Barone, Mario Pagliaro,* Cristina Della Pina,* Valeria Butera,* and Rosaria Ciriminna**

GrafeoPlad-Pd, a new metal-organic alloy comprised of Pd nanoparticles doped with 3D-entrapped graphene oxide, has promising applicative potential in sustainable synthetic organic chemistry. Besides hydrogenation, the metal nanopowder comprising the material is also active and relatively stable in cross-coupling reactions carried out consecutively. X-ray photoelectron spectroscopy (XPS) surface investigation and density functional theory (DFT) calculations are applied to gain new insight into the structure and potential new catalytic activity of this new class of molecularly doped metals.

1. Introduction

Recently introduced reporting the encapsulation of graphene oxide (GO) in palladium nanoparticles (or GO@nPd),[1] "GrafeoPlad" designates a new class of molecularly doped metals comprised of platinum group metals (PGMs) functionalized with 3D-entrapped graphene oxide molecules. The material, metal–organic alloy (MORAL),[2,3] should not be confused with composites comprised of palladium nanoparticles (NPs) deposited on the outer surface of graphene oxide (Pd/GO). Prepared via different surface heterogenization methods and chiefly applied as catalysts for synthetic organic chemistry, several reports describe the latter class of surface-decorated materials.[4–6] The 3D encapsulation of the graphene moiety in the lattice of palladium, on the other hand, makes use of Avnir's method for the entrapment of organic molecules in the lattice structure of metal crystals.[2,7]

The method is based on the direct reduction of the precursor metal ion in a solution containing the dissolved organic species followed by entrapment, aggregation, and precipitation. A MORAL indeed consists of an aggregate of metal crystallites (with typical particle sizes on the order of 100 μm) and interstitial porosity, with most dopant molecules residing on the metal crystallite surface in closed interstitial pores formed by the metal crystallite aggregation accessible to external reactants.[2,3,7] Recent insight on practical aspects concerning the use of MORALs in catalysis concluded that the reason explaining the low number of scholarly studies devoted to molecularly doped metals has to do with the difficulty of visualizing these materials.[8] For instance, the TEM photographs of GrafeoPlad-Pd (see below) show that the material is comprised of aggregated palladium nanoparticles, some of which clearly reveal the presence of GO layers on the edge of the aggregated nanoparticles, alongside Pd NPs intertwined with GO regions.[1] We now show that, besides hydrogenation, the metal nanopowder comprising GrafeoPlad Palladium is also active and relatively stable in mediating cross-coupling reactions. X-ray photoelectron spectroscopy (XPS) and density functional theory (DFT) calculations, furthermore, were used to gain new insight into the structure and potential new catalytic activity of this new class of molecularly doped metals.

2. Results and Discussion

The XPS survey spectra of the GrafeoPlad-Pd sample before and after catalysis are reported in **Figure 1**a,b, respectively. The presence of residual Cl and Zn used in the preparation of the GrafeoPlad was detected on the surface of the fresh sample (Figure 1a), along with the main C, O, and Pd photoelectron signals. The N 1s photoelectron peak in the survey of Figure 1b originates from the use of GrafeoPlad-Pd catalyst in nitrobenzene hydrogenation with hydrazine.[1] The XPS surface chemical composition of the investigated samples is listed in **Table 1**, wherein the elemental relative abundance is expressed as atomic percentage (at.%). After catalysis, a two-third reduction in the surface concentration of Pd is observed (from 15.5% to 3.1%) coherent with TEM images showing more exposed graphene oxide sheets, along with a substantial increase of carbon content (from 44.2% to 72.3%) and halving of oxygen concentration (from 37.0% to 18.6%) probably due to the reducing environment during the reaction.

M. Formenti, C. Della Pina
Dipartimento di Chimica
Università degli Studi di Milano
via Golgi 19, 20133 Milano, Italy
E-mail: cristina.dellapina@unimi.it

M. P. Casaletto, M. Pagliaro, R. Ciriminna
Istituto per lo Studio dei Materiali Nanostrutturati
CNR
via U. La Malfa 153, 90146 Palermo, Italy
E-mail: mariapia.casaletto@cnr.it; mario.pagliaro@cnr.it; rosaria.ciriminna@cnr.it

G. Barone, V. Butera
Dipartimento di Scienze e Tecnologie Biologiche
Chimiche e Farmaceutiche Università degli Studi di Palermo
v.le delle Scienze, Ed.17, 90128 Palermo, Italy
E-mail: valeria.butera@unipa.it

The ORCID identification number(s) for the author(s) of this article can be found under https://doi.org/10.1002/adsu.202300643

DOI: 10.1002/adsu.202300643

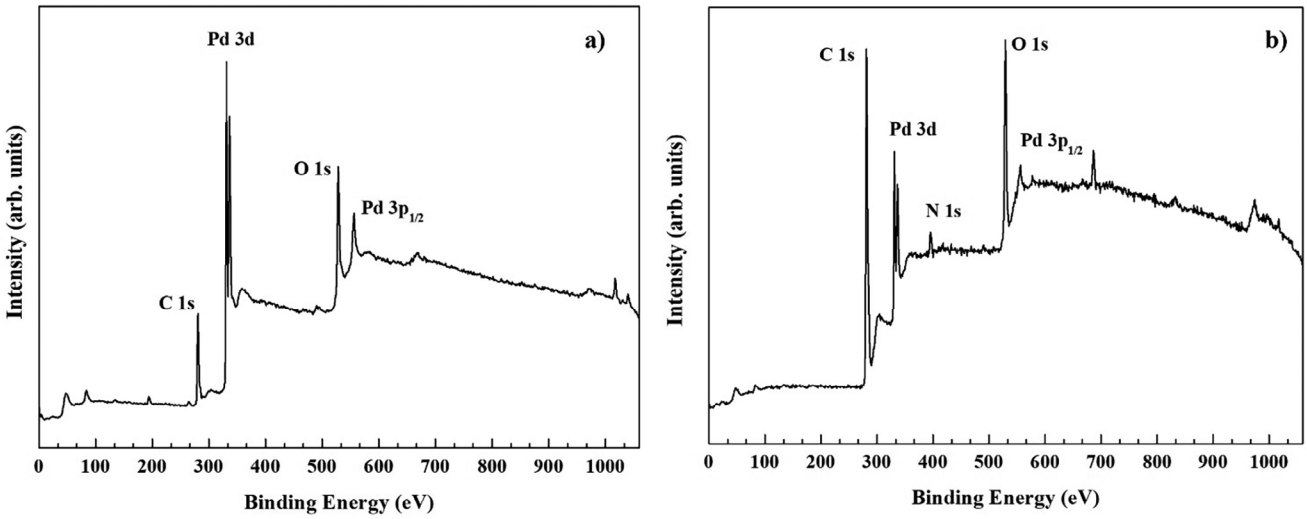

Figure 1. XPS survey spectra of the GrafeoPlad-Pd before (a) and after catalysis (b).

Table 1. XPS surface chemical composition of the investigated samples.

Sample[a)]	C 1s	Pd 3d	O 1s	N 1s	F 1s	Zn 2p	Cl 2p
GrafeoPlad-Pd (fresh)	44.2	15.5	37.0	–	–	1.8	1.5
GrafeoPlad-Pd (after catalysis)	72.3	3.1	18.6	2.6	3.1	0.3	–

[a)] Elemental concentration as an atomic percentage (at. %).

Table 2. XPS surface distribution of Pd species, resulting from the curve fitting of Pd 3d photoelectron signals (total peak area = 100%) in GrafeoPlad-Pd before and after employment as a catalyst in nitrobenzene reduction with excess hydrazine.

XPS peak	Pd 3d [eV]	Assignment	Peak area [%]
GrafeoPlad-Pd (fresh)	335.7–341.0	Pd	71.2
	336.9–342.2	PdO	28.8
GrafeoPlad-Pd (after catalysis)	334.5–339.8	Pd	82.5
	336.3–341.6	PdO	17.5

The high-resolution XPS Pd 3d, C1s, and O1s core level spectra were deconvoluted in order to study the element speciation on the GrafeoPlad-Pd surface. The curve-fitting analysis of the Pd 3d peak in the investigated samples is reported in **Figure 2** and the resulting surface distribution of Pd species is listed in **Table 2**. The photoelectron signal of Pd 3d consists of a Pd $3d_{5/2}$ and Pd $3d_{3/2}$ doublet, with well-separated spin-orbit components (Δ = 5.29 eV) in a 3/2 intensity ratio. The deconvolution of the Pd 3d spectrum in fresh GrafeoPlad-Pd in Figure 2a reveals a major Pd $3d_{5/2}$ component located at BE = 335.7 eV, originating from metallic Pd, and a second component at BE = 336.9 eV assigned to PdO, due the interaction of Pd and graphene oxide and/or to the surface partial oxidation of Pd nanoparticles.

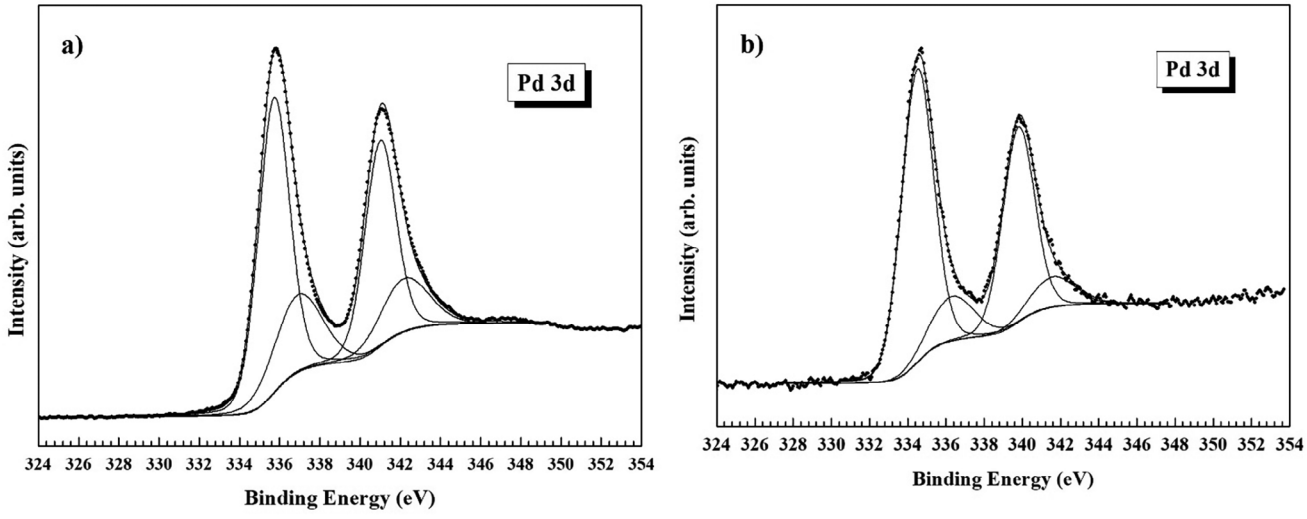

Figure 2. XPS curve-fitting of Pd 3d spectra in the GrafeoPlad-Pd before (a) and after catalysis (b).

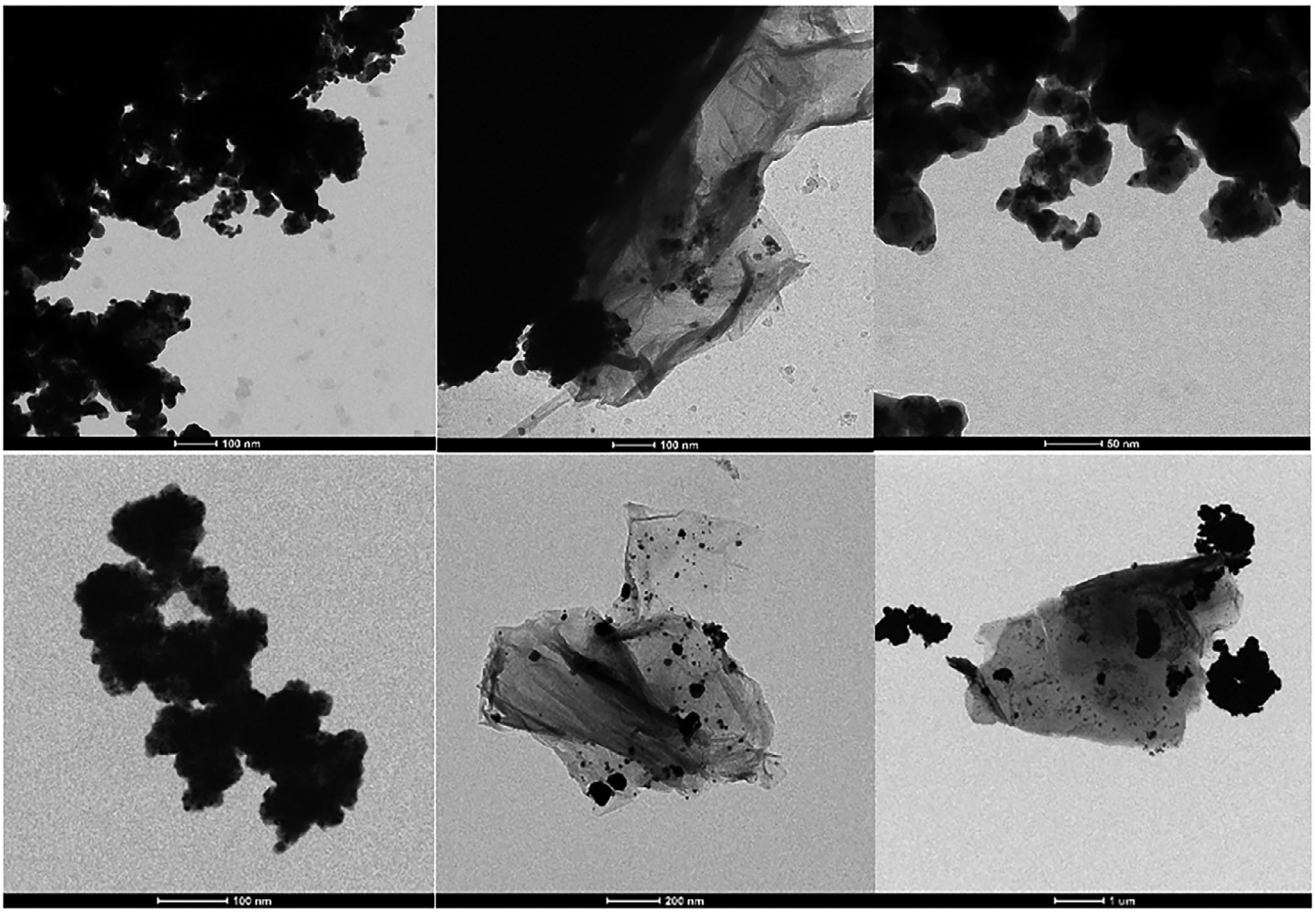

Figure 3. TEM photographs of fresh (top) and used (bottom) GrafeoPlad Pd.

The apparently significant decrease of metallic Pd content at the surface (see the surface elemental concentration as atomic percentage in Table 1) might be due to the leaching of palladium. However, we indirectly checked for leaching by assessing the catalytic activity of the filtrate in the hot-filtration test. Lack of activity, though observed, does not exclude that catalytically inactive Pd species are leached into the reaction mixture. However, the TEM photographs (see **Figure 3** below) and XRD profiles of the fresh and used GrafeoPlad material (not shown) indicate no change in the Pd nanoparticle average size prior to and after employment. Metal sintering indeed usually accompanies the leaching of soluble Pd species in solution. On the other hand, after catalysis, the Pd 3d spectrum of GrafeoPlad-Pd confirmed the existence of two chemical states of Pd on the surface (Figure 2b) with the lower binding energy component at BE = 334.5 eV assigned to metallic Pd and the higher binding energy component at 336.3 eV attributed to PdO.[9] The Pd $3d_{5/2}$ and $3d_{3/2}$ doublet at 334.5 eV for Pd metal and 336.5 eV for PdO in the XPS spectrum of Pd nanoparticles,[10] is shifted to 335.7 eV for Pd(0) and at 336.9 eV for PdO in the case of fresh GrafeoPlad-Pd (Table 2). After employment in reduction catalysis with excess hydrazine, the amount of metallic Pd increases from 71.2% to 82.5%, and that of PdO decreases from 28.8% to 17.5%. The signal for metal Pd, furthermore, shifts to 1.2 eV lower binding energy due to the fact that in metals like Pd in which the d-band is more than half full, the surface atoms acquire a net negative charge relative to the bulk which translates in a surface component in the Pd $3d_{5/2}$ signal appearing at lower binding energy.[10]

In addition, an increase in the size of the palladium NPs upon catalysis would translate into a negative shift of 3d core-level electrons.[11] However, we did not measure a change in the Pd nanoparticle average size prior to and after the employment of GrafeoPlad-Pd in nitrobenzene reduction catalysis via XRD analyses and after taking the TEM photographs (Figure 3). The latter also clearly unveils the presence of graphene oxide sheets prior to and after usage in catalysis.

The C 1s spectrum in all investigated samples was deconvoluted by four different components, as shown in **Figure 4**. The surface distribution of C species, resulting from the curve fitting of C 1s peak, is reported in **Table 3**.

The four C 1s components located at BE = 284.6, 285.6, 286.8, and 289,4 eV can be respectively assigned to the presence of surface sp^2-hybridized carbon atoms, sp^3-hybridized carbon atoms, C—O/C—OH groups, and carboxyl C═O groups.[12,13] Compared to the XPS signals of GO, with five peaks at 284.5, 285.6, 286.7, 287.7, and 289.0 eV corresponding, respectively, to C═C, C—OH, C—O, C═O, and HO—C═O C 1s photoelectrons characteristic for the particular groups of GO,[14] the high relative abundance of C-OH sp^3 carbons at the surface of Pd-entrapped GO and the low amount of carboxyl groups suggest that most latter groups in GO

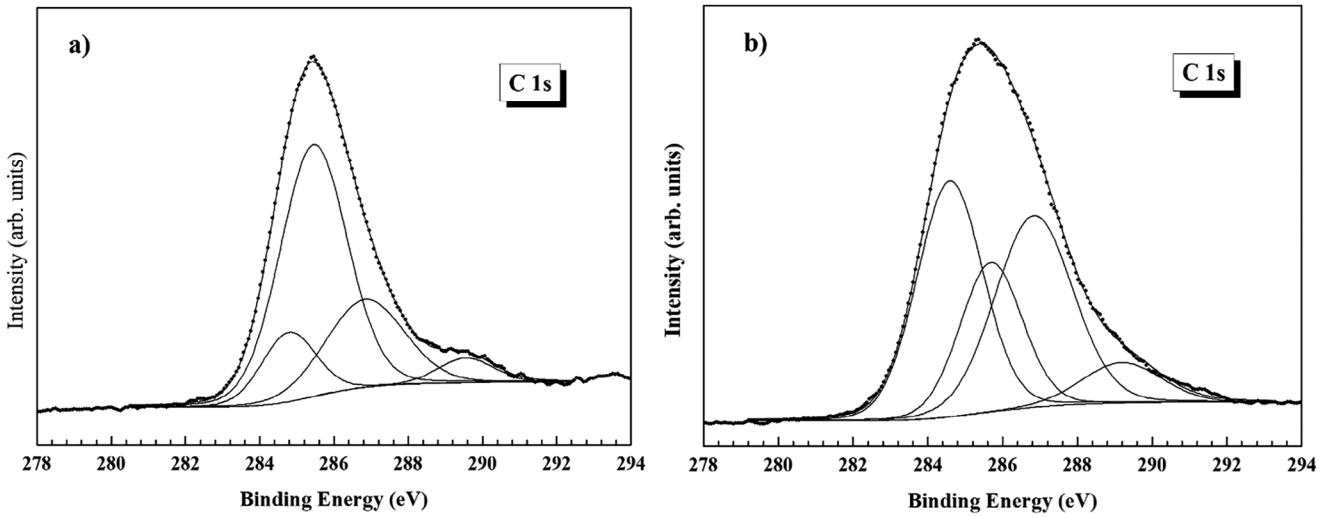

Figure 4. XPS curve-fitting of C 1s spectra in the GrafeoPlad-Pd before (a) and after catalysis (b).

Table 3. XPS surface distribution of C species, from the curve fitting of C 1s photoelectron signals (total peak area = 100%) in GrafeoPlad-Pd before and after employment as a catalyst in nitrobenzene reduction with excess hydrazine.

Binding energy C1s [eV] Assignment	284.6 C sp^2 [%]	285.6 C sp^3 [%]	286.8 C—O—C [%]	289.4 O—C═O [%]
GrafeoPlad-Pd fresh	13.0	58.4	23.8	4.8
GrafeoPlad-Pd after catalysis	7.5	36.1	34.7	21.7

are reduced during the reduction of Pd^{2+} with Zn leading to precipitation of the MORAL.[1]

Employment of the MORAL in nitrobenzene reduction with an excess of hydrazine[1] results in a substantial reduction and thus decrease of the C═C graphitic carbon bonds, and a concomitant decrease from 58.4% to 36.1% in the amount of C sp^3 carbons. The latter is accompanied with a nearly fivefold increase in the amount of carboxylic group at the surface of the material, from 4% to 21.7%. This counterintuitive and contradictory behavior can be explained by the ability of GO to act as an oxidation catalyst in the presence of oxygen dissolved in methanol during catalysis for certain C atoms in the GO structure,[15] while certain C—O-forms undergo reduction due to hydrazine. These hypotheses will be checked in future work.

In the case of the curve fitting of the O 1s spectrum, the direct overlap between the Pd $3p_{3/2}$ component located around BE = 534 eV and the O 1s peak should be considered. The Pd 3p region consists of a spin-orbit Pd $3p_{3/2}$ and a Pd $3p_{1/2}$ doublet, with well-separated components (BE = 17 eV). The presence of the Pd $3p_{1/2}$ component is well evidenced in the XPS survey spectra of the investigated samples (Figure 1a,b). The curve fitting of O 1s spectra for GrafeoPlad-Pd before (a) and after catalysis (b) is displayed in **Figure 5**, and the results are listed in **Table 4**. The O 1s spectrum can be deconvoluted in four components corresponding to oxide species as in PdO and/or O—C═O groups (530.5 eV); C═O groups (532.3 eV), C—OH and/or C—O—C groups (533.8 eV) and adsorbed water (535.4 eV). The component located at BE = 533.8 eV overlaps with Pd $3p_{3/2}$.

In order to gain further insight we carried out DFT calculations based on two different models. In the first model, GO is represented by coronene with 2 oxygen atoms below and above the graphitic plane, forming two epoxides. The Pd nanoparticles are simulated by adding a cluster of 3 Pd atoms above and below the coronene plane. The outcome of DFT calculations clearly indicates the formation of a chemical bond between Pd and C, whose distances are in the 2.14-2.18 Å range (**Figure 6**).

In Model II, two Pd atoms were added to the six present in Model I. The outcome of DFT calculations returned similar Pd—C bond distances when compared to the model with six Pd atoms. In Model II, however, one Pd atom steps away from the GO plane and forms a bonding interaction with the oxygen atom with a calculated distance of 2.33 Å from the oxygen atom of the epoxide (**Figure 7**). The HOMO/LUMO orbitals plot in Figure S1 (Supporting Information) suggests a lower orbital overlap when compared to Model I with six Pd atoms, though the interaction is still present and significant. In other words, increasing the size of the Pd nanoparticle weakens the Pd-GO interaction. The 3D entrapment of graphene oxide in the crystal lattice of Pd via the reductive precipitation method[1] is completely different from the 2D adsorption of Pd nanoparticles on GO also from the DFT viewpoint. In Pd/GO, for example, similar calculations suggest that Pd preferably binds the oxygen atoms of two neighboring epoxy groups forming two Pd—O bonds, with the Pd atom being strongly anchored through an O—Pd—O bridge with a Pd—O bond length of 1.97 Å.[16]

We thus applied the material as a catalyst of the Suzuki–Miyaura cross-coupling reaction between arylboronic (phenylboronic) acid and aryl halogenides (bromobenzene and iodobenzene). Results in **Table 5** show that GrafeoPlad-Pd is indeed a good catalyst for the coupling of iodobenzene whereas it shows less activity when attempting the coupling of bromobenzene with the boronic acid.

Table 4. XPS surface distribution of O species, from the curve fitting of O 1s photoelectron signals (total peak area = 100%) in GrafeoPlad-Pd before and after employment as a catalyst in nitrobenzene reduction with excess hydrazine.

Binding energy O1s [eV] Assignment	530.5 PdO/ O—C═O [%]	532.3 C═O [%]	533.8 C—O—C/C—OH [%]	535.4 Adsorbed water [%]
GrafeoPlad-Pd (fresh)	5.7	47.1	39.7	7.5
GrafeoPlad-Pd (after catalysis)	6.1	40.1	35.7	18.1

Due to the the stronger carbon halide bond determined by the higher halogen electronegativity (in the order Cl, 3.16 > Br, 2.96 > I, 2.66), the latter lower reactivity of bromobenzene is well-known and general for cross-coupling reactions.[17] Similarly, the fact that methanol is a far better reaction medium when compared to acetonitrile is due to the well-known need for protic solvents in the Suzuki–Miyaura reaction.[17] The kinetic profile of the Suzuki–Miyaura reaction in MeOH for iodobenzene cross-coupling shows (**Figure 8**, left) the typical sigmoidal shape, with a first rapid reaction rate within the first 40 min of reaction, followed by a substantially slower reaction in the second time period (1–3 h). While the reaction with iodobenzene proceeds nearly to completion, in the case of bromobenzene the yield reaches a maximum 56.4% value after which no further conversion of the substrate is observed. Catalyst reusability tests show unprecedented stability of the metallic GO@nPd powder toward sintering and deactivation. Indeed, the slow decrease in maximum conversion in consecutive reactions mediated by the same catalyst recovered and reused (Figure 8, right) should be compared to the complete deactivation of palladium black, namely Pd nanoparticle powder, after a single reaction run in many catalytic conversions from partial hydrogenation[18] through oxidation[19] reactions. Furthermore, clustering to form palladium black is the common deactivation mechanism of most cross-coupling reactions mediated by both homogeneous[20] and heterogeneous[21] Pd catalysts. In the latter case, very often substantial Pd nanoparticle aggregation and metal leaching occur, and the solid catalyst loses its activity in a Suzuki–Miyauara reaction after a single reaction run.[21]

The two most common poisoning reaction mechanisms that deactivate metallic palladium catalysts, indeed, either act by clustering the Pd atoms, clusters, and nanoparticles to metallic palladium microparticles of low surface area;[18,21] or, in oxidation reactions, via oxidation of the unprotected palladium black resulting in >20% of the metal being lost by dissolution into the reaction solvent.[19] In brief, the graphene moiety of the 3D-entrapped GO molecules stabilize the Pd nanoparticles against sintering as well as acting as electron donors, as clearly shown by the TEM and XRD analyses of GrafeoPlad-Pd before and after nitrobenzene catalytic reduction with excess hydrazine (showing no change in the Pd nanoparticle average size prior and after catalysis) as well as by the XPS analysis reported in this account. The latter shows that the signal for metallic Pd shifts to substantially (1.2 eV) lower binding energy, with the surface atoms acquiring a net negative charge.

3. Conclusion

In conclusion, the outcomes of new catalytic tests in cross-coupling reactions of GrafeoPlad-Pd, a metallic powder comprised of aggregated Pd nanoparticles doped with 3D-entrapped graphene oxide molecules, alongside the first XPS surface investigation and DFT calculations reveal the relevance of this new class of molecularly doped metal for sustainability.

Being a new catalytic material applicable to different reactions of large industrial relevance such as hydrogenation as cross-coupling reactions, the material is promising for green fine

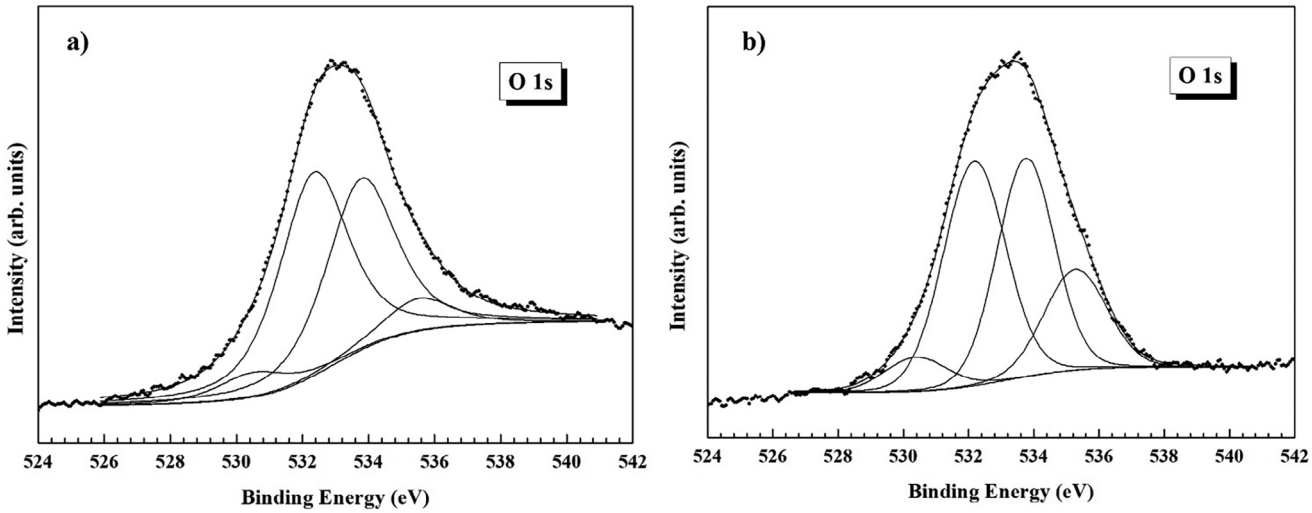

Figure 5. XPS curve-fitting of O 1s spectra in the GrafeoPlad-Pd before (a) and after catalysis (b).

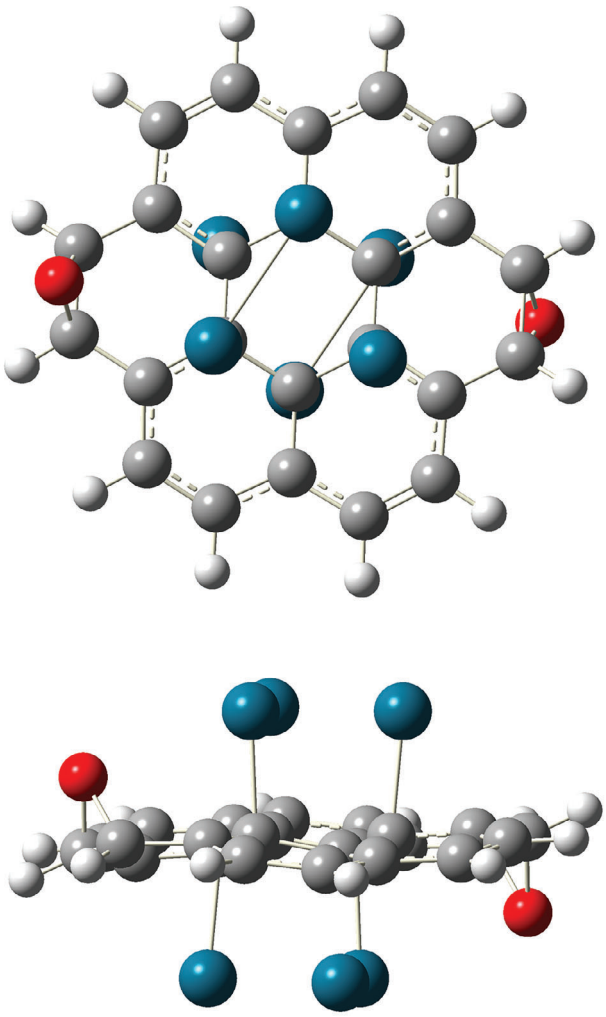

Figure 6. Model I used to mimic GrafeoPlad-Pd by DFT calculations: top and side view.

chemical productions.[22] The metallic GO@(nPd) nanoparticles, indeed, will be further deposited over large surface area materials regularly used as catalyst particle supports (sol–gel oxides, polymers, aluminas, silicas, metal–organic frameworks, etc.) dramatically lowering the amount of expensive Pd needed to catalyze the reaction and further improving the catalyst stability.

Table 5. Yield of the Suzuki–Miyauara coupling of phenilboronic acid and aryl halogenides mediated by GrafeoPlad-Pd in different aqueous solvent mixture.

Solvent[a]	Arylbenzene	Yield [%]
MeOH	Bromobenzene	56.4
	Iodobenzene	94.3
CH_3CN	Bromobenzene	31.6
	Iodobenzene	59.4

[a] Reaction conditions: organic solvent:water ratio 3:1, halobenzene 0.05 M, 1.2 eq. boronic acid, 4 eq. aqueous NaOH. Reaction mixture refluxed overnight.

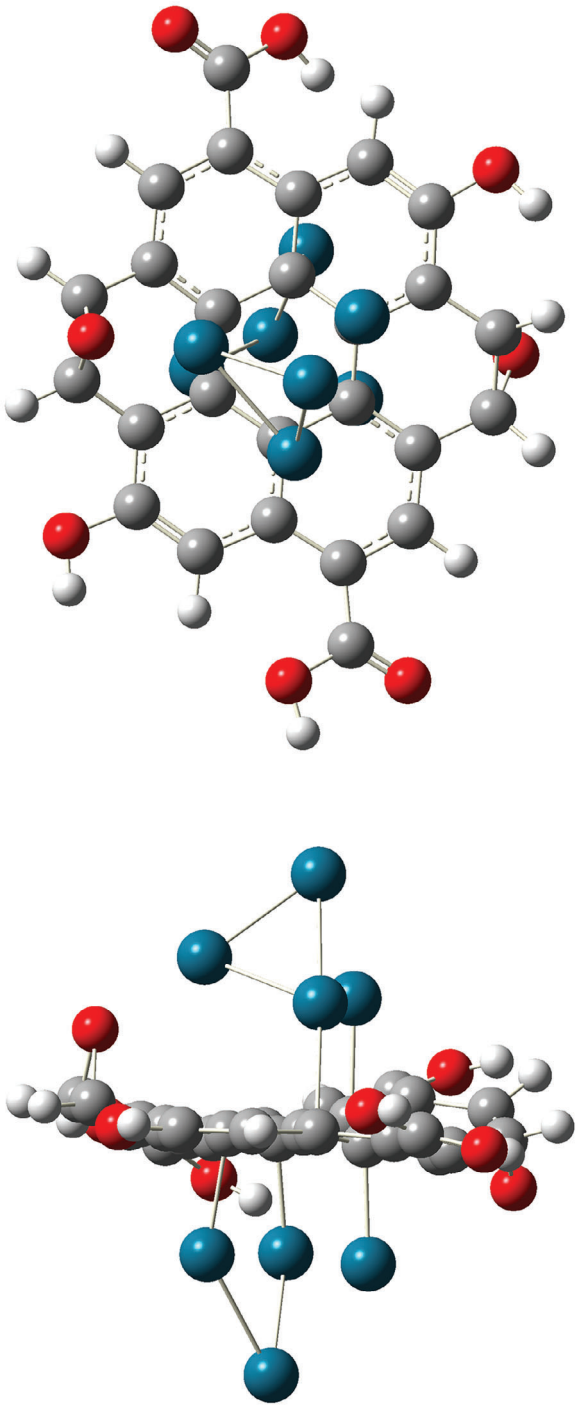

Figure 7. Model II used to mimic GrafeoPlad-Pd by DFT calculations: top and side view.

Heterogenization of GrafeoPlad catalytic materials belonging to PGMs over solid support, furthermore, will enable its application to a wide variety of conversions carried out continuously under flow.[23]

Ananikov and co-workers have extensively shown that acting in a "cocktail-type" manner, in catalytic processes mediated by Pd nanoparticles, single atoms, complex species, metal clusters,

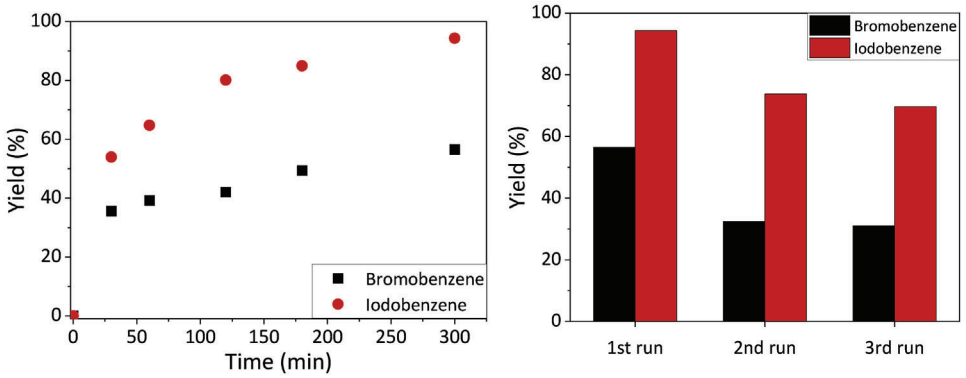

Figure 8. Progress of the Suzuki–Miyaura cross-coupling reaction between phenilboronic acid and aryl halogenides mediated by GrafeoPlad-Pd in methanol (left); reaction yield in three consecutive reaction runs mediated by the same GrafeoPlad-Pd catalyst recovered and reused (right).

and metal nanoparticles all actively take part in catalytic reaction cycles in nearly all cross-coupling reactions mediated by palladium.[24] In the case of Pd nanoparticles encapsulating the graphene moiety, the metal-organic alloy nature of the GO@(nPd) hybrid material should have profound consequences on its catalytic activity. Indeed, the first DFT calculations reported herein unveil the formation of a chemical bond between Pd and C, with the XPS surface investigation prior and after employment in reduction catalysis confirming the involvement in catalysis of both metallic Pd and PdO phases at the material surface, with a stabilizing role of the 3D-entrapped graphene moiety of the GO molecules against sintering. Forthcoming studies aimed to achieve the aforementioned progress will be based on the fundamental advances in understanding the nature of this new molecularly doped metal such as those reported in the present investigation.

4. Experimental Section

Catalytic Tests: GrafeoPlad-Pd was prepared as previously described.[1] In a typical Suzuki–Miyauara reaction, 2×10^{-4} mol of arylbenzene were dissolved in 3 mL of either methanol or acetonitrile selected as reaction solvent with phenylboronic acid (1.2 equivalents). The mixture was added with 1 mL aqueous NaOH (0.12 M) and the mixture was heated to reflux. Reaction progress was monitored via liquid chromatography with a Shimadzu LC-10AD VP HPLC equipped with a RID-10A detector and Restek Ultra BiPh 5 µm column (Restek, Cernusco Sul Naviglio, Italy) thermostated at 45 °C using a mixture H_2O:MeOH 65:35 + 0.1% v/v formic acid as eluent, flux 1 mL min^{-1}. At the end of the reaction, the catalyst was recovered by centrifugation, washed three times with methanol, and dried in the air.

XPS Surface Analysis and TEM Photographs: The transmission electron microscopy (TEM) experiments were carried out using a Thermo Fisher Scientific Talos L120C instrument operating at 120 kV as previously described in detail.[1] The surface analysis of the material was performed by XPS both before and after the catalytic hydrogenation of nitrobenzene with hydrazine at room temperature. The surface chemical composition was investigated with a Surface Sciences Instruments (SSI) M-Probe apparatus equipped with a monochromatic Al Kα source ($h\nu$ = 1486.6 eV). A spot size of 200 ÷ 750 µm and a pass energy of 25 eV was used during data acquisition. The constant charging of the binding energy scale (BE) was corrected by using the C 1s peak at BE = 284.6 eV from adventitious carbon as an internal reference. The position and full width at half-maximum (FWHM) of the C 1s line were carefully checked for every independent determination. The accuracy of the binding energy measure is ± 0.1 eV. Photoemission data were processed by using the XPSPeak free software for the analysis of XPS spectra written by Dr Raymund Kwok.[25] Data analysis was performed by a nonlinear least square curve-fitting procedure with a properly weighted sum of Lorentzian and Gaussian component curves, after background subtraction according to Shirley and Sherwood.[26] The assignment of photoelectron signals and peak components was determined according to the literature reference database.[9]

DFT Calculations: All DFT calculations were performed using the Gaussian 16[27] package. The cluster models were selected based on previous studies on similar systems.[28–30] The cluster's overall zero spin and neutral charge were retained by passivating with capping H atoms only those dangling C bonds of GO. The hybrid B3LYP[31,32] functional in conjunction with the SDD pseudo potential[33] for Pd atoms and the full electron basis sets 6–311G** for all the remaining atoms were selected. Frequency calculations have been done to check the nature of the stationary points.

Supporting Information

Supporting Information is available from the Wiley Online Library or from the author.

Acknowledgements

This work is dedicated to the memory of Professor Michele Rossi (1939–2023). The authors thank Manuela Gilberti and Marco Schiavoni, Università degli Studi di Milano, for the XPS measurements, and CINECA, the Italian supercomputing center, for providing the computational resources through the "IsB25_Andro17" grant. The authors thank the Università degli Studi di Milano PSR2021_DIP_005_PI_CDPIN project for funding.

Conflict of Interest

The authors declare no conflict of interest.

Data Availability Statement

The data that support the findings of this study are available from the corresponding author upon reasonable request.

Keywords

GrafeoPlad, graphene oxide, molecularly doped metal, MORAL, palladium

Received: December 14, 2023
Revised: January 23, 2024
Published online: March 17, 2024

[1] M. Formenti, M. Pagliaro, C. Della Pina, R. Ciriminna, *ChemRxiv.* **2023**, *15*, e202300600.
[2] D. Avnir, *Acc. Chem. Res.* **2014**, *47*, 579.
[3] G. Palmisano, V. Augugliaro, R. Ciriminna, M. Pagliaro, *Can. J. Chem.* **2009**, *87*, 673.
[4] S. Rostamnia, B. Zeynizadeh, E. Doustkhah, H. Golchin-Hosseini, *J. Colloid Interface Sci.* **2015**, *451*, 46.
[5] N. Shang, C. Feng, H. Zhang, S. Gao, R. Tang, C. Wang, Z. Wang, *Catal. Commun.* **2013**, *40*, 111.
[6] S.-i. Yamamoto, H. Kinoshita, H. Hashimoto, Y. Nishina, *Nanoscale.* **2014**, *6*, 6501.
[7] D. Avnir, *Adv. Mater.* **2018**, *30*, 1706804.
[8] R. Ciriminna, M. Formenti, M. Pagliaro, C. Della Pina, *ChemCatChem.* **2023**, *15*, e202300600.
[9] C. D. Wagner, J. W. Allison, J. R. Rumble Jr, A. V. Naumkin, A. Kraut-Vass, C. J. Powell, in *X-Ray Photoelectron Spectroscopy Database, (version 3.4)*, National Institute of Standards and Technology (NIST), Gaithersburg, MD **2003**.
[10] V. A. Bondzie, P. Kleban, D. J. Dwyer, *Surf. Sci.* **1996**, *347*, 319.
[11] K. Wertheim, S. B. DiCenzo, D. N. E. Buchanan, *Phys. Rev. B.* **1986**, *33*, 5386.
[12] R. Haerle, E. Riedo, A. Pasquarello, A. Baldereschi, *Phys. Rev. B.* **2001**, *65*, 045101.
[13] S. D. Gardner, C. S. K. Singamsetty, G. L. Booth, G.-R. He, C. U. Pittman, *Carbon.* **1995**, *3*, 587.
[14] L. Stobinski, B. Lesiak, A. Malolepszy, M. Mazurkiewicz, B. Mierzwa, J. Zemek, P. Jiricek, I. Bieloshapka, *J. Electron Spectrosc. Relat. Phenom.* **2014**, *195*, 145.
[15] D. R. Dreyer, A. D. Todd, C. W. Bielawski, *Chem. Soc. Rev.* **2014**, *43*, 5288.
[16] T.-T. Jia, C.-H. Lu, Y.-F. Zhang, W.-K. Chen, *J. Nanopart. Res.* **2014**, *16*, 2206.
[17] S. Akkoç, *J. Chin. Chem. Soc.* **2021**, *68*, 942.
[18] A. B. McEwen, M. J. Guttieri, W. F. Maier, R. M. Laine, Y. Shvo, *J. Org. Chem.* **1983**, *48*, 4436.
[19] M. Yu Berezin, K.-T. Wan, R. M. Friedman, R. G. Orth, S. N. Raman, S. V. Ho, J. R. Ebner, *J. Mol. Catal. A: Chem.* **2000**, *158*, 567.
[20] P. W. N. M. van Leeuwen, *Appl. Catal., A.* **2001**, *212*, 61.
[21] A. Kunfi, Z. May, P. Németh, G. London, *J. Catal.* **2018**, *361*, 84.
[22] S. Vásquez-Céspedes, R. C. Betori, M. A. Cismesia, J. K. Kirsch, Q. Yang, *Org. Process Res. Dev.* **2021**, *25*, 740.
[23] R. Ciriminna, M. Pagliaro, R. Luque, *Green Energy Environ.* **2021**, *6*, 161.
[24] A. S. Kashin, V. P. Ananikov, *J. Org. Chem.* **2013**, *78*, 11117.
[25] R. W. M. Kwok, *XPSPeak41, XPS Peak Fitting Program for WIN95/98, XPSPEAK Version 4.1*, Hong Kong, **2000**.
[26] P. M. A. Sherwood, D. Briggs, M. P. Seah, in *Data Analysis in X-ray Photoelectron Spectroscopy in Practical Surface Analysis by Auger and X-ray Photoelectron Spectroscopy*, Wiley, New York, USA **1990**.
[27] Gaussian 16, Revision C.01, M. J. Frisch, G. W. Trucks, H. B. Schlegel, G. E. Scuseria, M. A. Robb, J. R. Cheeseman, G. Scalmani, V. Barone, G. A. Petersson, H. Nakatsuji, X. Li, M. Caricato, A. V. Marenich, J. Bloino, B. G. Janesko, R. Gomperts, B. Mennucci, H. P. Hratchian, J. V. Ortiz, A. F. Izmaylov, J. L. Sonnenberg, D. Williams-Young, F. Ding, F. Lipparini, F. Egidi, J. Goings, B. Peng, A. Petrone, T. Henderson, D. Ranasinghe, et al., Gaussian, Inc., Wallingford CT, **2016**.
[28] R. K. Gupta, M. Malviya, K. R. Ansari, H. Lgaz, D. S. Chauhan, M. A. Quraishi, *Mater. Chem. Phys.* **2019**, *236*, 121727.
[29] V. Butera, H. Detz, *ACS Appl. Energy Mater.* **2022**, *5*, 4684.
[30] K. Karthick, T. K. Bijoy, A. Sivakumaran, A. B. Mansoor Basha, P. Murugan, S. Kundu, *Inorg. Chem.* **2020**, *59*, 10197.
[31] A. D. Becke, *J. Chem. Phys.* **1998**, *107*, 8554.
[32] A. D. Becke, *J. Chem. Phys.* **1998**, *98*, 5648.
[33] X. Y. Cao, M. Dolg, *J. Mol. Struct.* **2002**, *581*, 139.